Isogeometric Analysis Application to Car Crash Simulation

S. Bouabdallah[2], C. Adam[2,3], M. Zarroug[2], H. Maitournam[3]

[1]De Vinci Engineering Lab, École Supérieure d'Ingénieurs Léonard de Vinci
[2]Direction Scientifique et Technologies Futures, PSA Peugeot Citroën
[3]Laboratoire de Mécanique des Solides, École Polytechnique

Forum Teratec 2014 - July 2, 2014

ÉCOLE POLYTECHNIQUE ParisTech

ESILV LÉONARD DE VINCI

LMS

PSA PEUGEOT CITROËN

Outline

Industrial context

- Good predictive capability expected.
- Complete mesh size: $\simeq$ 3 million elements.

$\Longrightarrow$ Explicit simulations performed on the whole model.

- Stable time step: $\simeq 1\ \mu s$.
- 10 hours to simulate $\simeq 130ms$ on 96 CPUs.

$\Longrightarrow$ Excessive computational cost.

- $\geq 90\%$ of the geometry meshed with linear Reissner-Mindlin shell elements.

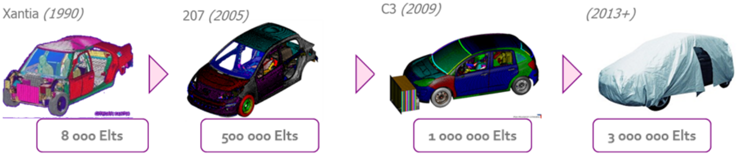

Figure: Model size evolution

Industrial context

- Geometry has proved to be very significant.
- Need to refine some components.

$\Longrightarrow$ Stable time step greatly penalized.

- Accurate and smooth geometry preferred for contact problems.
- Large time used for preparing and meshing parts.

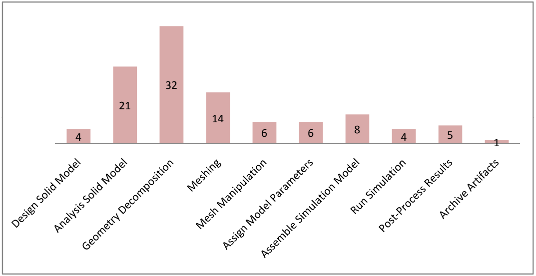

Figure: Estimation of relative time costs for model generation and analysis process

Industrial context

⟹ IsoGeometric Analysis for automobile crashworthiness.

- Parametrized CAD geometry for optimisation process.
- Analysis and Design share the same model.
- Higher regularity between elements within a patch.

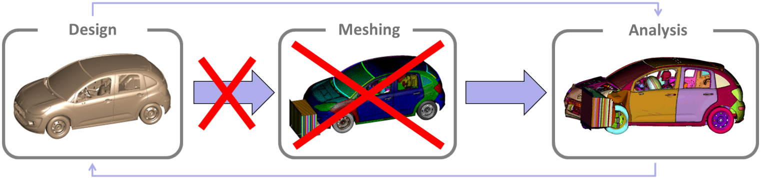

Figure: Numerical simulation process in isogeometric analysis.

Numerical locking

- Fully integrated low order elements, based on Timoshenko/Mindlin hypothesis, present poor performances with thin beams, plates and shells.
- Transverse shear and membrane locking appear.
- Classical Lagrange-based reduced and selective integration rules do not remove these pathologies.

$\Longrightarrow$ Need to define B-Spline/NURBS-based integration schemes.

Framework:

- Multi-patch problems with uniform regularity within each patch.
- Quadratic and cubic polynomials, regularity r from 0 to $p-1$.

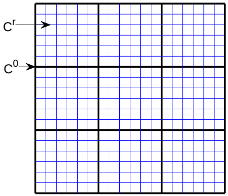

Pure bending problem

- Thick curved beam of length L and radius R clamped at one end.
- Moment of inertia for a rectangular section: $I = \frac{bh^3}{12}$.

- Distributed loading moment proportional to the bending stiffness:

$$m(s) = EI \left(\frac{\pi}{2L}\right)^2 \sin\left(\frac{\pi}{2L} s\right).$$

$\Longrightarrow$ Exact solution known, depends only of L and R:

$$u_n(s) \quad = \quad \frac{\frac{2L}{\pi}}{1-(\frac{2L}{\pi R})^2}\left(\cos\left(\frac{s}{R}\right) - \cos\left(\frac{\pi}{2L} s\right)\right).$$

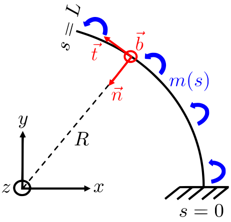

- Exact membrane and shear strains are zero.
- Severe test for membrane and shear locking.

Membrane and transverse shear locking

- One element with B-Splines of degree p from 1 to 5.
- Shear locking for slenderness ratio $L/h \gg 1$ and membrane locking for $L/h \gg R/L$.
- Both shear and membrane locking appear for all degrees p.

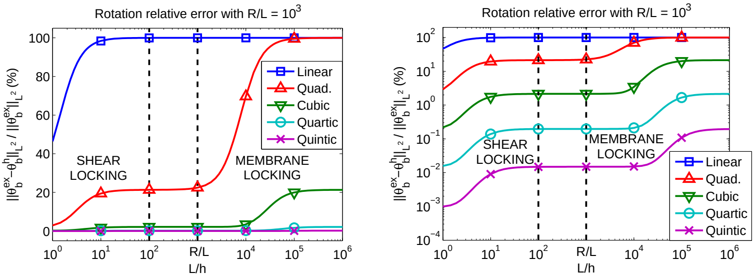

(a) Linear scale (b) Logarithmic scale

Figure: One element curved thick beam: rotation relative error in L^2 norm.

Transverse shear locking

- Different effects on convergence according to the couple (p, r).
- Degree 1: no pre-asymptotic convergence.
- Degree 2: slow pre-asymptotic convergence when C^0 and no pre-asymptotic convergence with few elements when C^1.
- Spurious constraints strengthened by the high regularity.

$\Longrightarrow$ Excessive bending stiffeness of the structure.

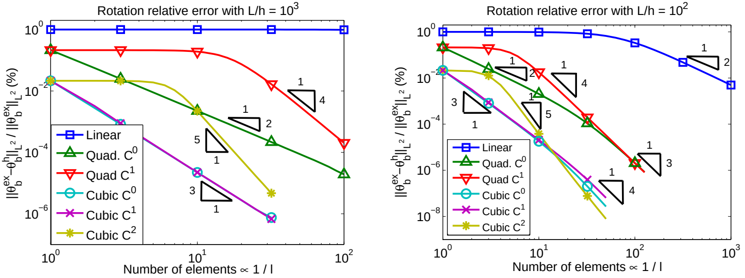

(a) Pre-asymptotic convergence with $L/h = 10^3$

(b) Pre-asymptotic and asymptotic convergence with $L/h = 10^2$

Mathematical framework

- Based on the work in FEA of [Prathap,93].
- Field-consistency paradigm in thick structural elements.
- Transverse shear strain in straight beam:

$$\gamma_s(s) \quad = \quad w_{,s}(s) - \theta(s).$$

- In the limit of an infinitely thin beam, the shear strain energy must vanish.

$\Longrightarrow$ Different physical and spurious constraints are obtained according to the couple (p,r).

- Mathematical induction is performed adding elements one-by-one.
- New unknowns and conditions are numbered.
- An over-constrained linear system leads to numerical locking whereas an under-constrained system produces zero energy modes.

1D B-Spline reduced quadrature rules

- Optimal selective reduced integration schemes adapted to high regularity basis functions.
- The higher the regularity is, the fewer Gauss points are needed.
- Shear and membrane locking are completely removed.
- Improved accuracy of curved beam B-Spline elements.

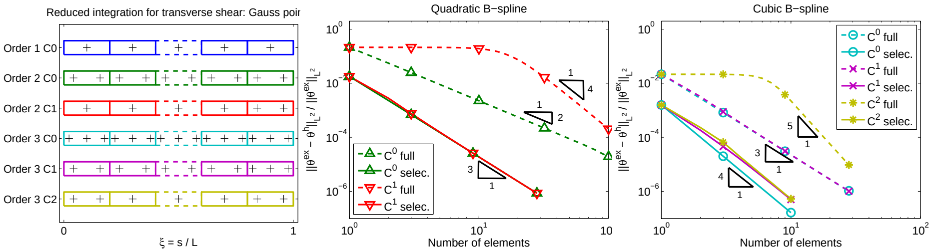

Figure: Rotation relative error in L^2 norm with full and selective reduced integrations.

Pure bending problem

- Same behaviours as with beams.
- High regularity wanted for more accurate results with fewer control points.
- Need to unlock B-Splines especially when C^{p-1} regularity.
- Possibility to extend integration rules from beams to plates and shells.

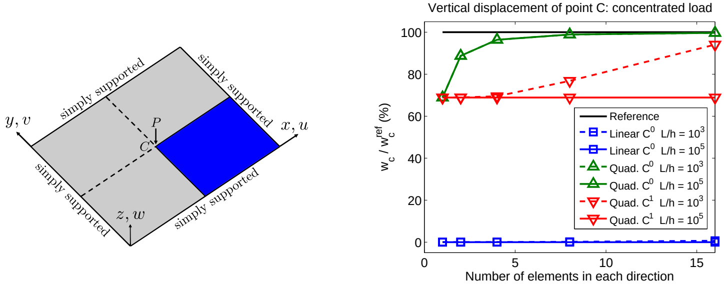

Figure: Central deflection of a simply supported plate (L/h $= 10^3$, 10^5).

Pure bending problem

- Same behaviours as with beams.
- High regularity wanted for more accurate results with fewer control points.
- Need to unlock B-Splines especially when C^{p-1} regularity.
- Possibility to extend integration rules from beams to plates and shells.

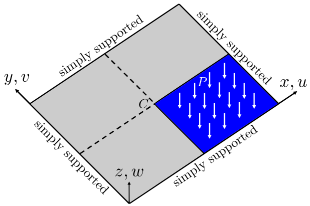

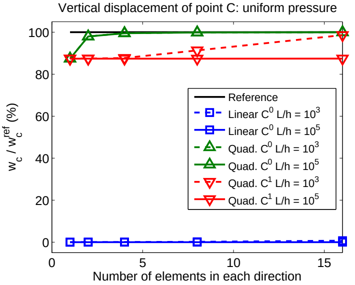

Figure: Central deflection of a simply supported plate (L/h $= 10^3$, 10^5).

2D B-Spline reduced quadrature rules

- Uni-dimensional B-Spline-based reduced quadrature rules extended to bi-dimensional rules by tensor product.
- The high regularity lowers the required number of Gauss points.
- Hourglass modes are suppressed using additional quadrature points in boundary elements, where the control points accumulate.

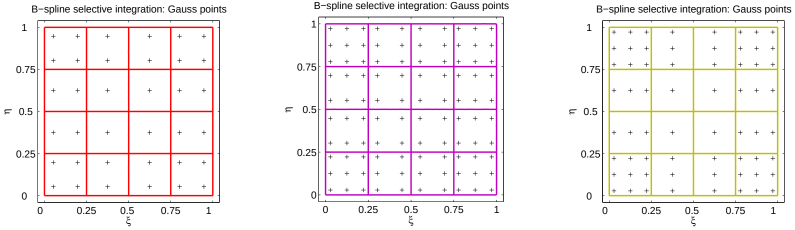

(a) Quadratic C^1 (b) Cubic C^1 (c) Cubic C^2

Figure: B-Spline selective integration quadrature rules and central deflection.

2D B-Spline reduced quadrature rules

- Resulting under-integrated elements are free from transverse shear locking.
- Numerical solutions independent of the thickness.
- Improved accuracy of plate isogeometric elements.
- No spurious zero energy modes.

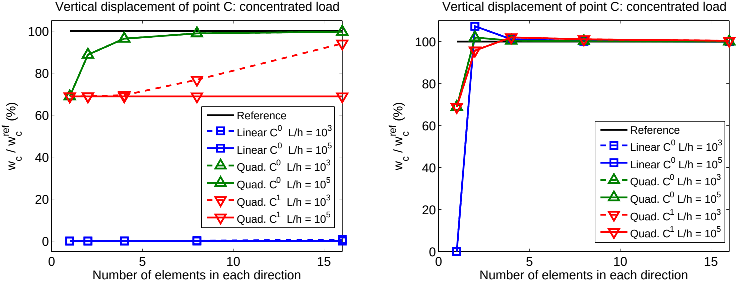

(a) Full integration (b) Reduced integration

Figure: Central deflection of a simply supported plate ($L/h = 10^3, 10^5$).

2D B-Spline reduced quadrature rules

- Resulting under-integrated elements are free from transverse shear locking.
- Numerical solutions independent of the thickness.
- Improved accuracy of plate isogeometric elements.
- No spurious zero energy modes.

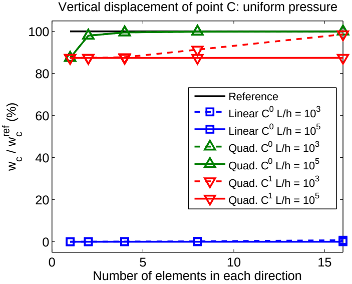

(c) Full integration

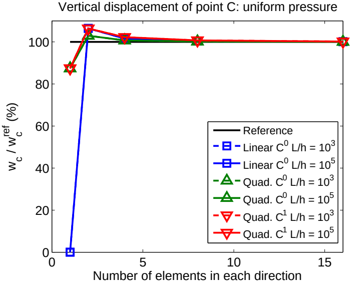

(d) Reduced integration

Figure: Central deflection of a simply supported plate ($L/h = 10^3$, 10^5).

Shell model

- Reissner-Mindlin shell model obtained from a degenerated three-dimensional model.
- First-order kinematic description through the thickness with transverse shear.
- Exact geometry of the shell defined by

$$\mathbf{x}(\boldsymbol{\xi}) = \sum_{A=1}^{nm} R_A(\xi,\eta)\mathbf{X}_A + \frac{h}{2}\zeta\mathbf{n}(\xi,\eta).$$

- Interpolated displacements described by

$$\mathbf{u}(\boldsymbol{\xi}) = \sum_{A=1}^{nm} R_A \left(\mathbf{U}_A + \frac{h}{2}\zeta\boldsymbol{\theta}_A \wedge \mathbf{n} \right).$$

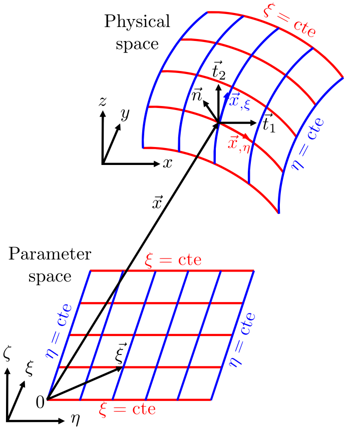

Characterization of the normal

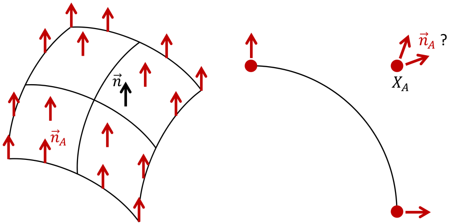

- Several possibilities:
  1. Exact normal:

$$\mathbf{n} = \frac{\mathbf{x}_{,\xi} \wedge \mathbf{x}_{,\eta}}{||\mathbf{x}_{,\xi} \wedge \mathbf{x}_{,\eta}||_2}.$$

  2. Collocated normal:

$$\mathbf{n} = \mathbf{n}_A \qquad \forall A \in [|1, nm|].$$

     a. $\mathbf{n}_A$ defined by the orthogonal projection of the associated control point $\mathbf{X}_A$ onto the mid-surface of the shell,
     b. $\mathbf{n}_A$ defined by a uniform distribution of the shell normals in the parametric space,
     c. $\mathbf{n}_A$ defined at the Greville abscissae in the parametric space.
- Exact normal formulation is incompatible with reduced integration.
- Collocation at Greville abscissae results in good compromise between accuracy and computation time.

Shell obstacle course problems

- Evaluate time efficiency and accuracy of the proposed under-integrated elements.
- Linear elasticity benchmark problems.
- Bending dominated problems: transverse shear and membrane locking.

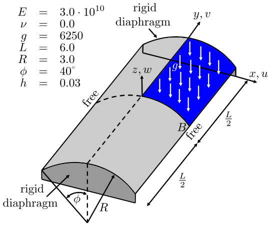

(a) Scordelis-Lo roof

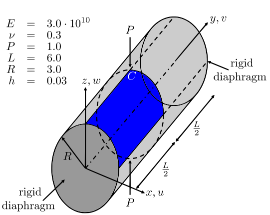

(b) Pinched cylinder

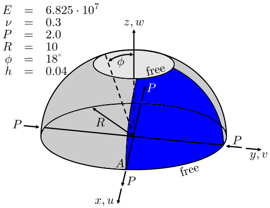

(c) Pinched hemisphere

Figure: The shell obstacle course: problem descriptions and data.

Accuracy

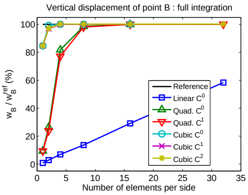

(a) Roof: full

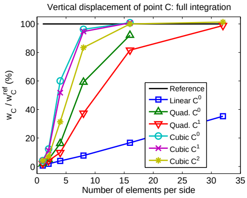

(b) Cylinder: full

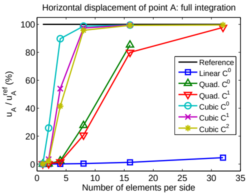

(c) Hemisphere: full

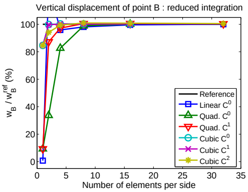

(d) Roof: reduced

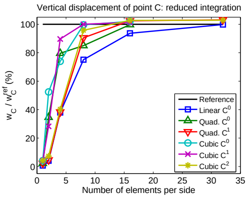

(e) Cylinder: reduced

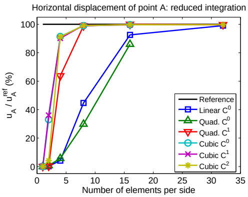

(f) Hemisphere: reduced

Figure: Shell obstacle course: displacement convergence

Time efficiency

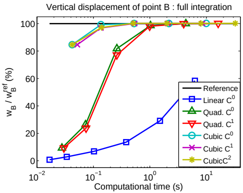

(a) Roof: full

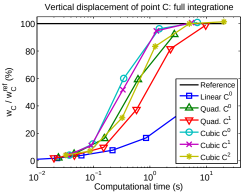

(b) Cylinder: full

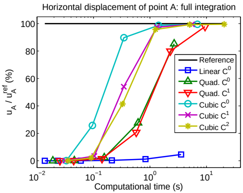

(c) Hemisphere: full

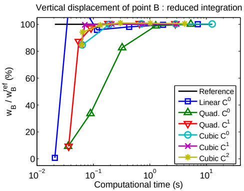

(d) Roof: reduced

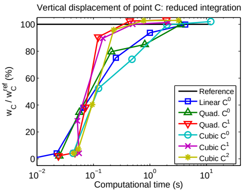

(e) Cylinder: reduced

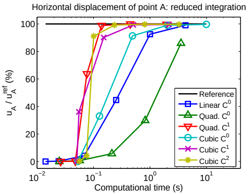

(f) Hemisphere: reduced

Figure: Shell obstacle course: displacement convergence

Total number of Gauss points

- Lagrange-based quadrature:

$$n_{\mathrm{GP}}^{\mathrm{bending}} = \left(e\left(\left\lceil \frac{2p+1}{2} \right\rceil\right)\right)^2 \text{ and } n_{\mathrm{GP}}^{\mathrm{shear}} = \left(e\left(\left\lceil \frac{2p+1}{2} \right\rceil - 1\right)\right)^2.$$

- B-Spline-based quadrature:

$$n_{\mathrm{GP}}^{\mathrm{bending}} = n_{\mathrm{GP}}^{\mathrm{shear}} = \left(e\left(\left\lceil \frac{2p+1}{2} \right\rceil - 1 - r\right) + 2r\right)^2.$$

- Computational effort depends on the difference $p - r$ when performing B-Spline-based reduced integration.
- Speed up factor greater than 5 (resp. 6) is reached with the under-integrated quadratic (resp. cubic) C^{p-1} elements.

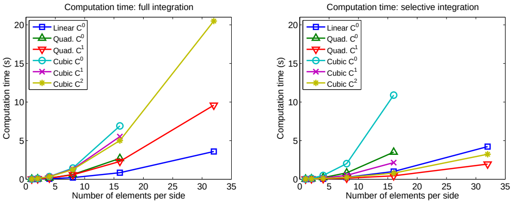

(a) Full integration (b) Selective integration

Figure: Computation time for the pinched cylinder problem.

Benchmark problems

- Solid-shell elements with one quadratic element in the thickness.
- Geometric non-linear elasticity benchmark problems.
- Bi-variate B-Spline-based quadrature rules applied.

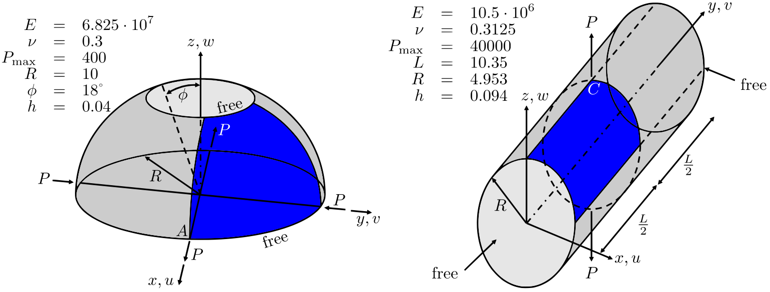

(a) Pinched hemisphere (b) Stretched cylinder

Figure: Geometric non-linear analysis of shells: problem descriptions and data.

Accuracy and time efficiency

- Bi-quadratic C^1 shape functions in the in-plane directions.
- Improved accuracy and time efficiency.
- Speed up factor of approximately 3.

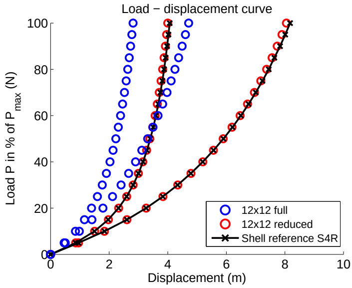

(a) Pinched hemisphere

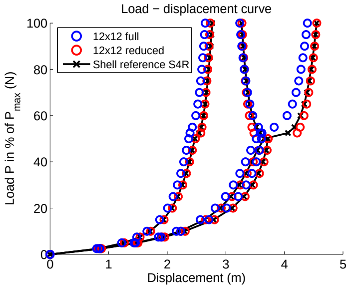

(b) Stretched cylinder

Figure: Displacement convergence with Total Lagrangian Formulation

Conclusions

- Severe numerical locking appear in quadratic and cubic C^{p-1} elements.

$\Longrightarrow$ Reduced integration to improve the performances of IG elements.

- Classical reduced/selective quadrature rules remove numerical locking in C^0 elements only.
- Mathematical framework to define B-Spline-based reduced 1D quadrature rules.
- Extension to 2D quadrature rules by tensor product.

$\Longrightarrow$ Efficient thick shell elements obtained as in FEA.

- Improved accuracy and time efficiency.
- Computational cost depends on the difference $p - r$.